

1 **Better together: Integrating and fusing multispectral and radar satellite**  
2 **imagery to inform biodiversity monitoring, ecological research and**  
3 **conservation science**

4

5 Henrike Schulte to Bühne<sup>1</sup>, Nathalie Pettorelli<sup>1\*</sup>

6 <sup>1</sup>Institute of Zoology, Zoological Society of London, Regent's Park, London NW1 4RY, UK

7 *Corresponding author: Nathalie Pettorelli, Institute of Zoology, Zoological Society of London,*  
8 *Regent's Park, London NW1 4RY, UK; email: [nathalie.pettorelli@ioz.ac.uk](mailto:nathalie.pettorelli@ioz.ac.uk); telephone: +44*  
9 *(0)207 4496334; fax: +44 (0)207 5862870.*

10

11 Authors' contributions: NP conceived the idea; HS carried out the literature research and  
12 led the writing of the manuscript, with regular inputs from NP. All authors contributed  
13 critically to the drafts and gave final approval for publication.

14 Number of words: 5602

15 Running headline: Satellite data fusion for ecology and conservation

16 Data accessibility: This paper does not use any data.

17

18 **Abstract**

19 1. The availability and accessibility of multispectral and radar Satellite Remote Sensing  
20 (SRS) imagery are at an unprecedented high. These data have both become standard source  
21 of information for investigating species ecology and ecosystems structure, composition and  
22 function at large scales. Since they capture complementary aspects of the Earth's surface,  
23 synergies between these two types of imagery have the potential to greatly expand  
24 research and monitoring opportunities. However, despite the benefits of combining  
25 multispectral and radar SRS data, data fusion techniques, including image fusion, are not  
26 commonly used in biodiversity monitoring, ecology and conservation.

27 2. To help close this application gap, we provide for the first time an overview of the most  
28 common SRS data fusion techniques, discussing their benefits and drawbacks, and pull  
29 together case studies illustrating the added value for biodiversity research and monitoring.

30 3. Integrating and fusing multispectral and radar images can significantly improve our  
31 ability to assess the distribution as well as the horizontal and vertical structure of  
32 ecosystems. Additionally, SRS data fusion has the potential to increase opportunities for  
33 mapping species distribution and community composition, as well as for monitoring  
34 threats to biodiversity. Uptake of these techniques will benefit from more effective  
35 collaboration between remote sensing and biodiversity experts, making the reporting of  
36 methodologies more transparent, expanding SRS image processing capacity and promoting  
37 widespread open access to satellite imagery.

38 4. In the context of a global biodiversity crisis, being able to track subtle changes in the  
39 biosphere across adequate spatial and temporal extents and resolutions is crucial. By

40 making key parameter estimates derived from SRS data more accurate, SRS data fusion  
41 promises to become a powerful tool to help address current monitoring needs, and could  
42 support the development of Essential Biodiversity Variables.

43

44 **Keywords:** Image fusion, object-level fusion, pixel-level fusion, remote sensing of  
45 biodiversity, satellite data fusion

46

## 47 **Introduction**

48 Satellite Remote Sensing (SRS) data from both radar and multispectral sensors have  
49 become a standard source of information for investigating species' ecology and ecosystems  
50 distribution and dynamics at large spatial scales (Buchanan et al. 2009; Pettoirelli et al.  
51 2014a). These two types of sensors acquire information about the Earth's surface in  
52 fundamentally different ways: whilst multispectral sensors passively measure  
53 electromagnetic radiation reflected from the Earth's surface, radar sensors are active,  
54 meaning they emit electromagnetic radiation and then measure the returning signal.  
55 Multispectral sensors capture information on chemical properties of surfaces, such as  
56 nitrogen or carbon content and moisture (Asner 1998; Tempfli et al. 2009), whereas radar  
57 responds to the three-dimensional structure of objects, being sensitive to their orientation,  
58 volume and surface roughness (Treuhaft et al. 2004). Additionally, radar sensors penetrate  
59 atmospheric conditions that incapacitate multispectral sensors, such as clouds, haze and  
60 fog, and can (depending on wavelength) return information from below the canopy  
61 (Santoro et al. 2007) or even from subsurface layers (McCauley et al. 1982). However, even  
62 though multispectral and radar sensors detect complementary aspects of the Earth's  
63 surface (Lahat et al. 2015), the two types of data are so far not routinely combined in  
64 biodiversity monitoring and ecological research.

65 To capitalise on the complementary characteristics of multispectral and radar sensors,  
66 their data needs to be integrated systematically, in a process generally called data fusion  
67 (Wald 1999). SRS data fusion can occur at three levels of analysis (Pohl & van Genderen  
68 1998; Fig. 1). First, imagery from different sensors can be used as separate predictors to

69 estimate a parameter of interest. This includes using multispectral and radar imagery  
70 jointly in a classification algorithm (Haack et al. 2002; Naidoo et al. 2016) or a statistical  
71 model (van der Wal & Herman 2007; Hamdan et al. 2014; Poggio & Gimona 2017). This is  
72 commonly referred to as *decision-level fusion*. Second, multispectral and radar imagery can  
73 be fused to derive entirely new predictors. This type of fusion includes *object-level fusion*, in  
74 which a landscape is divided into multi-pixel objects based on information from different  
75 remote sensors (Blaschke 2010), and *pixel-level fusion*, where pixel values are combined to  
76 derive a fused image with new pixel values, either in the spatial (Zhang 2010) or the  
77 temporal (Reiche et al. 2015a) domain. Since both pixel- and object-level fusions result in a  
78 new image, we will here refer to them as image fusion. When referring to decision-level  
79 fusion of SRS imagery, we will use the term “SRS data integration”, to emphasise that the  
80 SRS imagery remains separate. “SRS data fusion” refers to both SRS data integration and  
81 image fusion (Box 1).

82 The routine use of SRS data fusion in ecology and conservation science has been previously  
83 hampered by the need for intensive pre-processing, especially precise image co-  
84 registration (Pohl 1999). However, this obstacle has recently been removed with the  
85 launch of the ESA satellites Sentinel 1 and 2, which provide multispectral and radar  
86 imagery at high spatial and temporal resolutions, co-registered to sub-pixel accuracy,  
87 making these data suitable for direct use in SRS data fusion (Berger et al. 2012). As a result,  
88 there is now an unprecedented opportunity for ecologists and conservation scientists to  
89 capitalise on the opportunities associated with SRS data fusion. Whilst the benefits of data  
90 fusion for land cover and land use classification have recently been reviewed (Joshi et al.  
91 2016), there is currently no overview detailing its potential applications in ecology and

92 conservation. To address this literature gap, we here aim to (1) introduce relevant  
93 multispectral-radar SRS data fusion techniques, outlining their benefits and limitations, (2)  
94 illustrate situations where multispectral-radar SRS data fusion adds value over using a  
95 single source of data, and (3) outline existing limitations to the widespread use of SRS data  
96 fusion in ecology and conservation science, and discuss how these can be overcome.  
97 Because the application of multispectral-radar SRS data fusion in biodiversity monitoring is  
98 relatively new, we here aim to provide an overview over the variety of possible  
99 applications and opportunities arising from it, rather than present a systematic literature  
100 review.

101

## 102 **Overview of multispectral-radar SRS data fusion techniques, their benefits and** 103 **limitations**

104 A wide variety of pixel- and object-level techniques for multispectral-radar SRS data fusion  
105 exists (Pohl & Yen 2014; Fig. 2), each with specific advantages and weaknesses.

106 *Pixel- or observation-level fusion* occurs when corresponding pixel values from  
107 multispectral and radar images are combined to produce a new pixel value (Zhang 2010;  
108 Fig. 2), which is then used in the subsequent analysis instead of the original multispectral  
109 and radar values. Pixel-level fusion reduces the amount of information available later on,  
110 meaning that relevant patterns could be lost (Zhang 2010), but further processing can be  
111 significantly sped up because data volume is reduced. One further issue with this type of  
112 fusion is that it can lead to the production of new variables that can be difficult to interpret  
113 and relate to ecologically meaningful entities.

114 There are three main classes of pixel-fusion techniques: Component substitution, multi-  
115 resolution analysis and arithmetic (or modulation-based) techniques (Zhang 2010).

116 (1) *Component substitution techniques* such as principal component analysis (PCA)  
117 (Yonghong 1998; Fu et al. 2017) and intensity-hue-saturation (IHS) transformation  
118 (Chen et al. 2003; Leung et al. 2014) are among the most widely used pixel-fusion  
119 techniques (Pohl & Yen 2014). During PCA fusion, the original pixel values extracted  
120 from the radar and multispectral images are used to define new axes along which  
121 data variability is maximised; the new, fused pixel values are essentially linear  
122 combinations of their position along these new axes (Amarsaikhan et al. 2012). PCA  
123 image fusion is the only pixel-level image fusion technique that cannot be applied to  
124 imagery with different spatial resolutions. It is also the only pixel-level fusion  
125 technique that allows a theoretically unlimited number of multispectral and radar  
126 images to be fused; others typically limit this number to four (Pohl & van Genderen  
127 1998). IHS fusion represents another type of component substitution technique for  
128 pixel-level fusion, whereby three images with lower spatial resolution (typically  
129 multispectral data) are integrated with a single image with high spatial resolution  
130 (typically radar; Zhang 2010; Lu et al. 2011) to retain the radiometry but increase  
131 the spatial resolution of the former. Since the resulting images can be combined into  
132 a single RGB image, IHS fusion can facilitate visual interpretation (Zhang 2010). This  
133 process is similar to pansharpening, in which multispectral imagery with high  
134 spatial resolution is used to “sharpen” multispectral imagery with low spatial  
135 resolution, whilst maintaining the spectral information of the latter.

136 (2) *Multi-resolution analysis*, such as wavelet transformation (Zhang 2010; Lu et al.  
137 2011; Wang et al. 2016), is another broad type of pixel-level fusion, which starts  
138 with the decomposition of multispectral and radar imagery into their respective  
139 low- and high-frequency components (Lu et al. 2011). The wavelet transform of an  
140 image with low spatial resolution (typically multispectral) is used to replace the  
141 low-frequency transform of imagery with a higher spatial resolution (typically  
142 radar) before the fused image is reconstituted from the combined transforms.  
143 Wavelet transformations typically require a lot of computational resources for  
144 processing (Pohl & Yen 2014), but tend to be better at preserving the radiometry of  
145 the imagery with the lower spatial resolution than component substitution  
146 techniques such as PCA and IHS (Lu et al. 2011; Pohl & Yen 2014).

147 (3) *Arithmetic fusion techniques* such as the Brovey transform algorithm (Zhang  
148 2010) and high pass filtering (HPF; Zhang 2010; Lu et al 2011) are techniques  
149 occasionally used in pixel-level SRS image fusion (Pohl & Yen 2014). They involve  
150 combining the original pixel values of high and low spatial resolution imagery in a  
151 linear expression to “sharpen” imagery with low spatial resolution (Zhang 2010; Lu  
152 et al. 2011). Arithmetic fusion techniques do not deal well with imagery from  
153 different types of sensors, because they are based on the assumption that pixel  
154 values in the fused image are linear combinations of those in the original images  
155 (Zhang 2010), which may not be the case when combining multispectral and radar  
156 SRS data. Additionally, they do not typically perform well if there is a small or no  
157 difference in spatial resolution between the images to be fused (Zhang 2010). As a



158 result, arithmetic fusion techniques are unlikely to be appropriate for multispectral-  
159 radar SRS image fusion.

160 *Object-or feature-level fusion* means that objects such as lines, shapes or textures are  
161 extracted from radar and multispectral imagery, based on brightness and intensity values  
162 of each pixel, as well as its spatial context, which are then used in subsequent analyses  
163 (Zhang 2010). Under our definition of image fusion, this includes two techniques: First,  
164 multispectral and radar SRS images with the same spatial resolution can be fused via image  
165 segmentation, during which they are used jointly to split an area of interest into  
166 homogeneous, discrete and contiguous objects (Blaschke 2010; Fig. 2). This is the most  
167 commonly used object-based image analysis technique (Blaschke 2010). Second, objects  
168 can be extracted separately from multispectral and radar SRS data (of the same or different  
169 spatial resolution) and combined in a feature map, which is then used in subsequent  
170 analyses (Lisini et al. 2011). Object-based fusion reduces all multispectral and radar  
171 information into a single layer of discrete objects, which are often relatively easy to relate  
172 to ecological features. As a result, object-level fusion may facilitate the mapping of non-  
173 overlapping land cover classes because it reduces the number of objects that have to be  
174 classified. By contrast, pixel-based methods may be more suitable for mapping variables  
175 that vary significantly at spatial scales smaller than a given object, since they preserve the  
176 unique spectral and radar signal for each pixel.

177 *Decision-level fusion*, or SRS data *integration*, does not require an additional processing  
178 step; rather, SRS imagery from different sensors are combined as separate predictors in a  
179 quantitative decision-making framework – such as a regression, a quantitative model or a

180 classification algorithm. Since SRS data integration is spatially explicit, it requires the same  
181 accurate co-registration and pre-processing as SRS image fusion techniques.

182 The SRS data fusion techniques detailed above are typically used separately (e.g. Lu et al.  
183 2011); however, the development of hybrid techniques is an active research field, adding to  
184 the large choice of available techniques (Souza-Filho et al. 2009; Pohl & Yen 2014). The  
185 quality of information obtained through data fusion can vary significantly depending on the  
186 choice of the technique to be used (or combinations of techniques, e.g. Waske &  
187 Benediktsson 2007; Lisini et al. 2011; Lu et al. 2014; Wang et al. 2016). Since there is no  
188 coherent framework to choose the optimal technique given the large range of data types  
189 and applications, the current best practice is to test several different fusion methods on a  
190 representative subset of the area of interest, to gauge which approach may give the best  
191 results.

192

### 193 **Benefits for ecology, biodiversity research and conservation science**

194 Biodiversity is here defined as the structural, compositional and functional diversity of life,  
195 at different levels of organisation, including the genetic, species/population, and ecosystem  
196 levels (Noss 1990). Applications of multispectral-radar SRS data fusion (both image fusion  
197 and data integration) in biodiversity monitoring, ecology and conservation have the  
198 potential to improve the estimation of a wide range of key parameters, including 1) species  
199 distribution and community composition, 2) ecosystem distribution and structure, and 3)  
200 threats to biodiversity (Box 1; see Table 1A for case studies using image fusion, Table 1B  
201 for case studies for SRS data integration).

202 *Species distribution and community composition*

203 Species distribution and community composition are central topics in macroecology,  
204 biogeography, conservation science and environmental management (Myers et al. 2000;  
205 McDowall 2004; Keith et al. 2012). Species is here understood as a group of organisms  
206 sharing a unique, fixed set of heritable traits that allows them to be distinguished from  
207 other such groups (Cracraft 1987, Sangster 2014), whilst a community is defined a set of  
208 species co-occurring at a given time and place (McGill et al. 2006).

209 If a species of interest significantly affects the reflectance or backscatter signal received by  
210 a sensor, its distribution can be mapped directly from SRS (He et al. 2015). Whilst Light  
211 Detection and Ranging (LiDAR) and hyperspectral imagery (Box 1) is often recommended  
212 for mapping species directly, especially trees (e.g. Jones et al. 2010, Dalponte et al. 2012,  
213 Alonzo et al. 2014, Gosh et al. 2014), it is not possible (at present) to scale up these efforts  
214 to regional or continental scales, and systematically repeat them, since there are currently  
215 no active spaceborne LiDAR or hyperspectral missions. Due to the relatively coarse spatial  
216 resolution of most freely available multispectral and radar imagery (Fig. 3), direct species  
217 detection using this type of information has thus been mostly limited to mapping relatively  
218 large, homogenous stands of plants (e.g. Bradley & Mustard 2006, Gavier-Pizarro et al.  
219 2012). In this context, multispectral-radar imagery fusion has the potential to improve  
220 mapping of sufficiently large stands of plants with subtly different growth forms or  
221 phenology. For instance, Hong and colleagues (2014) were able to map stands of alfalfa  
222 *Medicago sativa* in grasslands by fusing radar backscatter (from the RADARSAT-2 sensor)  
223 and multispectral radiance (from the MODIS sensor) via IHS transformation, essentially

224 pan-sharpening the MODIS imagery before classification. This image fusion improved  
225 overall distribution mapping accuracy by 11% and 20% compared to using multispectral  
226 and radar data alone, respectively. The complementary strengths of multispectral and  
227 radar sensors can also be exploited by integrating them at the decision level to support  
228 species distribution mapping efforts. For instance, Ghulam et al. (2014) mapped three  
229 invasive plant species in a tropical forest by combining multispectral-derived information  
230 on vegetation type (from IKONOS and Geo-Eye-1) and radar-derived information on  
231 canopy structure (from ALOS PALSAR/RADARSAT-2) in a decision tree framework. The  
232 authors did not quantify how integrating these SRS data affected mapping accuracy  
233 compared to using a single data source, but they did report that the detection of one of the  
234 species was not possible based on multispectral SRS alone.

235 Indirect species mapping is based on the principle that remotely sensed variables reflect  
236 habitat conditions that in turn are related to species distribution (He et al. 2015). Usually,  
237 rather than fusing imagery, multispectral and radar SRS data are integrated as distinct  
238 predictor variables in species distribution models. For bird species in particular, vertical  
239 habitat structure is important (Bergen et al. 2009), and may be better captured by radar  
240 backscatter than more indirect parameters derived from multispectral SRS, such as forest  
241 cover (Buermann et al. 2008; Culbert et al. 2013). For instance, Bergen et al. (2007) found  
242 that integrating radar-derived biomass information with vegetation type derived from  
243 multispectral SRS data increased the accuracy with which the distribution of bird species  
244 could be predicted. A similar approach has been used to predict the distribution of trees  
245 species across South America, using the Leaf Area Index (LAI) and the Normalised  
246 Difference Vegetation Index (NDVI) data (both derived from multispectral SRS; Box 1) in

247 combination with canopy moisture and roughness metrics derived from radar data (Prates-  
248 Clark et al. 2008). Notably, in some of the above examples, the size of the study area was  
249 several million square kilometres (Table 1), illustrating the potential offered by SRS data  
250 fusion for large-scale habitat mapping.

251 Compared to direct and indirect monitoring of species, SRS data fusion has rarely been  
252 applied to support the monitoring of communities. One exception to this pattern is the  
253 study by Wolter & Townsend (2011), who mapped the relative basal area of different tree  
254 species in a temperate forest after fusing multispectral and radar imagery (Landsat  
255 TM/SPOT-5 and RADARSAT-1/ALOS PALSAR respectively). In this particular situation, SRS  
256 image fusion improved the accuracy with which community composition was estimated,  
257 likely because the sensors had complementary strengths in detecting different tree species.

258

### 259 *Ecosystem distribution and structure*

260 Changes in ecosystem distribution and condition is at the heart of ecosystem accounting  
261 (UNSD SEEA-EEA 2013; Mace et al. 2015), and plays an important role in ecosystem risk  
262 assessments (Nicholson et al. 2009) such as the Red List of Ecosystems (Keith et al. 2013).  
263 Ecosystem here refers to a community, an associated abiotic environment, the interactions  
264 among and between them, and the physical space in which they interact (Tansley 1935;  
265 Pickett & Cadenasso 2002). SRS data fusion has been used to estimate a wide range of  
266 parameters informing the distribution of ecosystems, as well as parameters related to the  
267 horizontal and vertical structure of ecosystems (Table 1).

268 Ecosystem distribution

269 Multispectral-radar SRS data fusion generally increases land cover classification accuracy  
270 (Joshi et al. 2016), allowing the separation of subtly different land cover types. This is  
271 relevant for biodiversity monitoring where it allows distinguishing between different types  
272 of ecosystems, vegetation types or geomorphological structures. Integrating multispectral  
273 and radar data at the decision level has been shown to increase accuracy of forest type  
274 mapping. SRS data integration has been mainly applied in tropical rainforests (e.g. Laurin  
275 et al. 2013), though such efforts have also been successful in temperate regions (e.g.  
276 Hégart-Masclé et al. 1998, Polychronaki et al. 2014, Barrett et al. 2016). This is likely  
277 because multispectral and radar sensors respond to different characteristics of forest  
278 stands: whilst multispectral data picks up on differences in vegetation “greenness”, radar  
279 backscatter contains information about canopy volume, and thus helps distinguish  
280 different stages of regrowth, or structurally distinct plantations from natural forests (e.g.  
281 Dong et al. 2013). This point is well illustrated by Rignot and colleagues’ work (1997) in the  
282 Amazon, which combined forest maps derived from Landsat 5 TM and SIR-C radar imagery  
283 to distinguish primary from secondary forest, as well as several regrowth stages. The  
284 combined approach allowed distinguishing a higher number of forest categories at high  
285 accuracy than using either data type alone. In some cases, image fusion can have additional  
286 benefits over SRS data integration: Lu and colleagues (2014) for example argue that  
287 multispectral-radar SRS image fusion (Landsat TM and ALOS PALSAR L-band respectively)  
288 enables a better distinction between different stages of tropical forest succession than is  
289 achieved by integrating the same SRS data using a classification algorithm. Fusion of  
290 multispectral with longwave radar in particular facilitates mapping succession stages in

291 tropical forests (Lu et al. 2011), potentially because it penetrates the canopy to a greater  
292 degree than shortwave radar (Baghdadi et al. 2009). Similarly, Morel et al. (2012) reported  
293 that effectively combining multispectral and radar at the *post-decision* stage (i.e. combining  
294 maps derived from each sensor separately) is less effective than SRS image fusion or data  
295 integration for improving forest detection accuracies.

296 In addition to forest mapping, wetland mapping efforts can benefit from multispectral-  
297 radar synergies, mostly via object-level image fusion (Table 1; but see Bwangoy et al. 2010  
298 for an example of multispectral-radar SRS data integration applied to tropical wetlands).  
299 The rationale for combining multispectral and radar imagery for wetland monitoring is  
300 that radar imagery allows the mapping of surface water or wet soils, even beneath a  
301 canopy (Bourgeau-Chavez et al. 2009), whilst multispectral data responds to vegetation  
302 and wetness in open canopies. Multispectral-radar image fusion has been used to  
303 distinguish between geomorphological structures in wetlands (Hamilton et al. 2007, Souza-  
304 Filho et al. 2009), or different vegetation types (Bourgeau-Chavez et al. 2009, 2016).  
305 However, these studies did not compare mapping accuracy achieved after image fusion to  
306 that achieved by using a single type of sensor, so it is unclear what the added value of  
307 image fusion was in these cases. Some insights are provided by Fu et al. (2017), who found  
308 that fusing ALOS-PALSAR/RADARSAT-2 and multispectral imagery from GF-1 increased  
309 mapping accuracy of wetland vegetation types beyond that achieved by using these data on  
310 their own. Similarly, when multispectral and radar imagery (Landsat TM5 and ALOS  
311 PALSAR, respectively) were integrated in a classification tree modelling approach,  
312 misclassification of different types of wetland vegetation and the extent of standing water  
313 were significantly reduced (Ward et al. 2014). Nevertheless, benefits of multispectral-radar

314 SRS data fusion may vary by wetland class (Maillard et al. 2008; Robertson et al. 2015) or  
315 with patch size (Gala & Melesse 2012).

316

317 Horizontal structure

318 Apart from enabling a better assessment of ecosystem and vegetation type distributions,  
319 integrating multispectral and radar imagery can also support efforts to estimate  
320 continuous parameters that characterise horizontal ecosystem structure related to canopy  
321 or soil structure. Horizontal ecosystem structure is here understood as the horizontal  
322 arrangement of ecosystem components in space (Bergen et al. 2009). Naidoo et al. (2016)  
323 for example reported that woody canopy cover is more accurately estimated when adding  
324 ALOS PALSAR and Landsat TM to a Random Forest algorithm (instead of using ALOS  
325 PALSAR on its own). Similarly, Cartus et al. (2011) successfully mapped tree stem density  
326 across 1,5 mio km<sup>2</sup> of forest using on ERS-1 and 2 imagery and the MODIS Vegetation  
327 Continuous Field product. Multispectral-radar SRS data integration has also helped map  
328 sediment grain size in intertidal flats (van der Wal & Herman 2007), as well as soil  
329 properties such as moisture (Wang et al. 2004) and chemical or physical composition  
330 (Poggio & Gimona 2017).

331

332 Vertical structure

333 Estimating the vertical structure of ecosystems, which refers to the vertical arrangement of  
334 ecosystem components in space (Bergen et al. 2009), can be facilitated by SRS image fusion  
335 and data integration. So far, the focus has been on forest ecosystems and monitoring



336 biomass, as demonstrated by Basuki and colleagues (2013) who used multispectral-radar  
337 image fusion to assess aboveground biomass in tropical forests. Others have derived  
338 biomass from integrating multispectral and radar data in quantitative (Wang & Qi 2008) or  
339 empirical (Hyde et al. 2006, Ismail et al. 2015) models. Hyde et al. (2006) found that whilst  
340 LiDAR does provide more accurate estimates of canopy height and biomass on its own,  
341 integrating multispectral and airborne (X-band) radar data could achieve comparable  
342 accuracies, much higher than that achieved by either sensor type alone. This result is  
343 echoed by Hamdan et al. (2014) and Attarchi & Gloaguen (2014), who both used  
344 spaceborne L-band radar to estimate biomass in tropical and temperate forests  
345 respectively. This suggests that integrating or fusing multispectral and radar imagery could  
346 provide an important opportunity to improve biomass monitoring in the absence of a  
347 spaceborne LiDAR sensor. Apart from estimating biomass, multispectral and radar imagery  
348 have been fused to monitor forest height (Walker et al. 2007; Kelldorfer et al. 2010) with  
349 moderate accuracy ( $R^2$  between 0.7 and 0.9) when validated against forest inventory or  
350 LiDAR-derived samples of forest height. However, since these studies did not explicitly  
351 compare the accuracy of their models with and without data fusion, it is unclear to which  
352 extent combining the data types benefited them.

353

#### 354 *Threats to biodiversity*

355 Being able to detect threats to biodiversity at all levels of biological and ecological  
356 organisation is necessary to prioritise areas for conservation (Joppa et al. 2016), plan  
357 conservation interventions (Pressey & Botrill 2008; Tulloch et al. 2015) and understand

358 the processes that shape biodiversity across a landscape (Shea et al. 2004). So far, SRS data  
359 fusion has rarely been applied to detect threats to biodiversity, but some promising case  
360 studies have emerged, mainly mapping deforestation across medium-sized study areas  
361 (hundreds or thousands of square kilometres, Table 1). It's worth mentioning here that  
362 deforestation mapping has a different focus than forest distribution assessments:  
363 deforestation mapping aims to optimise the identification of areas where trees have been  
364 removed by humans, whereas forest mapping seeks to optimise the assessment of forest  
365 extent, often aiming to distinguish between different forest types (e.g. successional stages,  
366 Lu et al. 2011, 2014), and/or quantify forest condition.

367 Combining multispectral and radar imagery has been shown to improve deforestation  
368 monitoring and reduce the lag between a deforestation event and its detection in areas  
369 where multispectral SRS data have significant cloud gaps (Asner 2001; Lehmann et al.  
370 2011; Reiche et al. 2015a,b). Reiche and colleagues (2015a) for example fused time series  
371 of multispectral and radar information at the pixel level, using the correlation between  
372 overlapping multispectral and radar time series to predict missing values in the former;  
373 this yielded a fused image for each time step, which was used to track deforestation. They  
374 reported that image fusion increased the overall accuracy with which deforestation was  
375 detected by 2.4% (compared to using only multispectral SRS data) under less cloudy  
376 conditions, but that, as cloud cover increased, this improvement in accuracy increased to  
377 ca. 40%. Additionally, the lag between deforestation events and their detection was  
378 significantly reduced, which makes these analyses more useful for informing responses on  
379 the ground.

380 Integrating multispectral and radar SRS data acquired at (roughly) the same time can help  
381 simultaneously reduce data gaps from cloud cover (for multispectral SRS) and layover (for  
382 radar SRS, Reiche et al. 2013), as well as improve the ability to distinguish forest from  
383 other land cover classes (Lehmann et al. 2011), both of which facilitates deforestation  
384 detection. By contrast, integrating subsequent multispectral and radar images in a Bayesian  
385 decision-framework has given mixed results: Whilst Lehmann et al. (2015) report that  
386 switching between SRS data types (here: from Landsat to PALSAR) increases erroneous  
387 detection of deforestation, Reiche et al. (2015b) found higher deforestation detection  
388 accuracy, and a reduction in detection lag, when integrating these SRS data sets. Forest  
389 degradation is another key threat to forest biodiversity which could benefit from fusing  
390 multispectral and radar SRS data. Forest degradation can either be detected through  
391 changes in forest structure, composition and function; it is also possible in some instances  
392 to map discrete degradation categories. For instance, integrating backscatter from ALOS  
393 PALSAR and tasselled cap-transformed Landsat 5 TM imagery in a Random Forest  
394 classification framework helped distinguish different stages of palm swamp degradation  
395 (Hergoualc'h et al. 2017).

396 Compared to species- and ecosystem-level biodiversity monitoring multispectral-radar SRS  
397 data fusion has been applied to a relatively small range of biodiversity threats (Table 1),  
398 but four potential further avenues are worth mentioning. First, SRS data fusion has been  
399 shown to improve the accuracy with which indicators of eutrophication – such as Secchi  
400 depth – can be estimated across large areas (Zhang et al. 2002, Liu et al. 2014). This  
401 suggests that SRS data fusion could be a useful tool for monitoring threats to freshwater  
402 and marine ecosystems which are under pressure from anthropogenic eutrophication, such

403 as coastal areas (e.g. Kemp et al. 2005). Second, Stroppiana and colleagues (2015) reported  
404 that integrating radar imagery from Envisat ASAR and multispectral imagery from Landsat  
405 5 TM in a fuzzy decision framework improved burned area mapping. Though it is not  
406 possible to distinguish anthropogenic and wildfires from space, this suggests that SRS data  
407 fusion could support monitoring changes in fire dynamics, which threaten biodiversity in  
408 many ecosystems (Enright et al. 2015). Third, the detection of infrastructure associated  
409 with anthropogenic threats to biodiversity, such as roads, may benefit from SRS data  
410 fusion. Integrating LiDAR information about three-dimensional structure of landscapes  
411 with multispectral imagery has been shown to improve road detection over using  
412 multispectral imagery alone (Hu et al. 2004). Given the current lack of a satellite-based  
413 LiDAR mission, however, radar imagery could be used to provide similar information about  
414 the vertical structure of surfaces, and could be fused with multispectral imagery to  
415 facilitate road mapping (Lisini et al. 2011). Fourth, multispectral-radar synergies could  
416 help improve the mapping of invasive plant species, which may differ from native species  
417 in spectral characteristics (reflected in spectral reflectance), as well as growth and volume  
418 patterns (reflected in radar backscatter; Ghulam et al. 2014). Whether and to which degree  
419 data fusion can improve the detection of these anthropogenic threats however remains to  
420 be tested.

421

422 **What currently limits wider use of data fusion techniques?**

423 Multispectral-radar SRS data fusion can have significant added value over using  
424 multispectral and radar SRS data alone, but there are currently four challenges that could  
425 prevent its routine use.

426 First, there is a lack of understanding of the contexts in which multispectral-radar SRS data  
427 fusion likely improves estimates, which makes it difficult for scientists to decide where to  
428 invest time and energy in additional processing and analysis. There are indeed contexts in  
429 which multispectral-radar SRS data fusion does not improve accuracy over using a single  
430 type of SRS data, or in which the benefits of fusion depend on the type of multispectral and  
431 radar data used (Ban 2003), the fusion technique (Lisini et al. 2011; Basuki et al. 2013;  
432 Hong et al. 2014; Wang et al. 2016) or (in the case of classifications) which land cover class  
433 and/or which time period is considered (Polychronaki et al. 2014; Robertson et al. 2015;  
434 Carreiras et al. 2017). Collaboration between the ecology/biodiversity and the remote  
435 sensing communities, via platforms like the Group on Earth Observations Biodiversity  
436 Observation Network, will be crucial in identifying which biodiversity parameters could  
437 benefit most from SRS data fusion approaches, and which datasets and processing  
438 techniques are most appropriate (Pettorelli et al. 2014b).

439 Second, multispectral-radar image fusion is often used without reporting a reason for data  
440 selection or fusion techniques, so it is hard to learn from experience. Additionally, it is often  
441 difficult to report all data analysis steps to a reproducible level of detail. A key step towards  
442 improving the transparency of SRS data fusion is making the code used in such analyses  
443 accessible, e.g. by using open-source software (Fig. 2). Scientific workflow systems, such as

444 Kepler (Ludäscher et al. 2009), could also help make SRS fusion methods more transparent,  
445 and aid quick identification and uptake of useful approaches (Michener & Jones 2012).

446 Third, data fusion requires the capacity, both in terms of hardware and analysis skills, to  
447 source and process two very different types of SRS data. Barriers to more widespread use  
448 of SRS data by ecologists in general – such as unfamiliar data formats, pre-processing  
449 requirements, or lack of appropriate hardware (Kuenzer et al. 2014) – are multiplied when  
450 using two different types of data. Even among ecologists and biodiversity researchers  
451 which routinely use SRS data, self-reported data handling proficiency tends to be lower for  
452 active sensors such as radar (Palumbo et al. 2017). The added value of multispectral-radar  
453 SRS data fusion may well outweigh these technical drawbacks in many cases, but will  
454 clearly present an obstacle for widespread adoption in a scientific community that is still in  
455 the process of embracing big data (Michener & Jones, 2012). However, the emergence of  
456 cloud computing (e.g. in the Google Earth Engine), and growing coding literacy amongst  
457 ecologists could help minimise the impact of this obstacle (Marvin et al. 2016). Moreover,  
458 many open-source software platforms already have tools supporting common data fusion  
459 techniques, reducing the entry barrier to a more widespread uptake (Fig. 1).

460 Fourth, data accessibility can remain a significant obstacle to multi-sensor SRS data fusion.  
461 Whilst multispectral SRS data, notably from the Landsat mission, have been freely available  
462 for almost a decade (Wulder et al. 2012), open access radar data has been more restricted,  
463 although ESA's Sentinel missions are likely to alleviate this data accessibility problem  
464 (Turner et al. 2015; Fig. 3). To fully take advantage of multispectral-radar data fusion  
465 opportunities, especially for time series analysis, accessibility to past acquisitions is

466 necessary. As a result, promoting open-access data policies for current and future missions  
467 as well as data archives remains important (Turner et al. 2015).

468

## 469 **Conclusion**

470 SRS data fusion allows taking advantage of the complementary information captured by  
471 different sensors (Lu et al. 2014; Joshi et al. 2016), and has the potential to increase the  
472 quality of SRS-derived parameters for ecology and conservation. The case studies  
473 presented here are entry points for more structured efforts to benefit from the growing  
474 availability of multi-satellite data. There are currently many SRS missions with an open-  
475 access policy providing global and repeated coverage of the Earth's surface, both for  
476 multispectral and radar data (Fig. 3). This offers the unique opportunity to scale up SRS  
477 image fusion and integration to large spatial scales, and support global biodiversity  
478 monitoring efforts. These efforts are currently centred on the concept of Essential  
479 Biodiversity Variables (EBVs) (Pereira et al. 2013), which are variables that allow  
480 quantification of the rate and direction of change in one aspect of the state of biodiversity  
481 over time and across space (Pettorelli et al. 2016). SRS variables have been identified as a  
482 key resource to produce EBVs (so-called SRS-EBVs; Pettoirelli et al. 2016), mainly for  
483 variables relating to ecosystem structure and function (Geijzendorfer et al. 2016, Pettoirelli  
484 et al. 2017). So far, however, development of SRS-EBVs and other variables for large-scale  
485 biodiversity monitoring has been largely focused on using SRS data from a single sensor  
486 (e.g. Pasher et al. 2013, Vihervaara et al. 2017). Whilst multispectral and radar SRS data  
487 fusion has mainly been applied to structural or compositional aspects of biodiversity, it

488 could also benefit monitoring of functional aspects. For instance, mapping wetland  
489 inundation extent (e.g. Ward et al. 2014), forest succession stage (e.g. Lu et al. 2011), or  
490 burned areas (Stroppiana et al. 2015), and monitoring water quality (Zhang et al. 2002, Liu  
491 et al. 2014), have all been shown to benefit from multispectral-radar synergies, allowing  
492 more accurate characterisation of related ecosystem processes and functions (such as  
493 water and disturbance regulation and primary productivity). Identifying how SRS data  
494 fusion could support global biodiversity monitoring efforts through SRS-EBVs requires  
495 collaboration between remote sensing scientists and biodiversity/ecology scientists (Fig.  
496 4). Each community's expertise and experience will be required to match monitoring  
497 requirements to remote sensing capability, so that SRS-EBVs are relevant, cost-effective  
498 and their production feasible (Pettorelli et al. 2016). This process will be particularly  
499 important for exploring the as-yet untapped opportunities arising from SRS data fusion to  
500 expand our biodiversity monitoring options from space. Much remains to be discovered  
501 about how best to capitalise on recent technological developments and changes in SRS data  
502 availability; we hope this contribution, by providing a solid introduction to SRS data fusion  
503 and its benefits for ecology and conservation, paves a way for this.

504



505 **References**

506 Amarsaikhan, D., Saandar, M., Ganzorig, M., Blotevogel, H. H., Egshiglen, E., Gantuyal, R.,  
507 Nergui, B. & Enkhjargal, D. (2012), Comparison of multisource image fusion methods and  
508 land cover classification. *International Journal of Remote Sensing*, **33**, 2532-2550.

509

510 Asner, G. P. (1998), Biophysical and biochemical sources of variability in canopy  
511 reflectance. *Remote sensing of Environment*, **64**, 234-253.

512

513 Asner, G. P. (2001), Cloud cover in Landsat observations of the Brazilian Amazon.  
514 *International Journal of Remote Sensing*, **22**, 3855-3862.

515

516 Attarchi, S., & Gloaguen, R. (2014). Improving the estimation of above ground biomass  
517 using dual polarimetric PALSAR and ETM+ data in the Hyrcanian mountain forest (Iran).  
518 *Remote sensing*, **6**, 3693-3715.

519

520 Baghdadi, N., Boyer, N., Todoroff, P., El Hajj, M., & Bégué, A. (2009). Potential of SAR sensors  
521 TerraSAR-X, ASAR/ENVISAT and PALSAR/ALOS for monitoring sugarcane crops on  
522 Reunion Island. *Remote Sensing of Environment*, **113**, 1724-1738.

523

524 Ban, Y. (2003), Synergy of multitemporal ERS-1 SAR and Landsat TM data for classification  
525 of agricultural crops. *Canadian Journal of Remote Sensing*, **29**, 518-526.

526

527 Barrett, B., Raab, C., Cawkwell, F., & Green, S. (2016), Upland vegetation mapping using  
528 Random Forests with optical and radar satellite data. *Remote Sensing in Ecology and*  
529 *Conservation*, **2**, 212-231.

530

531 Basuki, T. M., Skidmore, A. K., Hussin, Y. A., & Van Duren, I. (2013). Estimating tropical  
532 forest biomass more accurately by integrating ALOS PALSAR and Landsat-7 ETM+ data.  
533 *International journal of remote sensing*, **34**, 4871-4888.

534

535 Bergen, K. M., Gilboy, A. M., & Brown, D. G. (2007). Multi-dimensional vegetation structure  
536 in modeling avian habitat. *Ecological Informatics*, **2**, 9-22.

537

538 Bergen, K. M., Goetz, S. J., Dubayah, R. O., Henebry, G. M., Hunsaker, C. T., Imhoff, M. L., ... &  
539 Radeloff, V. C. (2009). Remote sensing of vegetation 3-D structure for biodiversity and  
540 habitat: Review and implications for lidar and radar spaceborne missions. *Journal of*  
541 *Geophysical Research: Biogeosciences*, **114**.

542

543 Berger, M., Moreno, J., Johannessen, J. A., Levelt, P. F., & Hanssen, R. F. (2012), ESA's sentinel  
544 missions in support of Earth system science. *Remote Sensing of Environment*, **120**, 84-90.

545

546 Blaschke, T. (2010), Object based image analysis for remote sensing. *ISPRS journal of*  
547 *photogrammetry and remote sensing*, **65**, 2-16.

548

549 Bourgeau-Chavez, L.L., Riordan, K., Powell, R.B., Miller, N. & Nowels, M. (2009) Improving  
550 Wetland Characterization with Multi-Sensor, Multi-Temporal SAR and Optical/Infrared  
551 Data Fusion. In: *Advances in Geoscience and Remote Sensing*, Gary Jedlovec (Ed.), InTech,  
552 DOI: 10.5772/8327.

553

554 Bourgeau-Chavez, L. L., Endres, S., Powell, R., Battaglia, M. J., Benscoter, B., Turetsky, M., ... &  
555 Banda, E. (2016). Mapping boreal peatland ecosystem types from multitemporal radar and  
556 optical satellite imagery. *Canadian Journal of Forest Research*, **47**, 545-559.

557

558 Bradley, B. A., & Mustard, J. F. (2006). Characterizing the landscape dynamics of an invasive  
559 plant and risk of invasion using remote sensing. *Ecological Applications*, **16**, 1132-1147.

560

561 Buchanan, G. M., Nelson, A., Mayaux, P., Hartley, A., & Donald, P. F. (2009), Delivering a  
562 global, terrestrial, biodiversity observation system through remote sensing. *Conservation*  
563 *Biology*, **23**, 499-502.

564

565 Buermann, W., Saatchi, S., Smith, T. B., Zutta, B. R., Chaves, J. A., Milá, B., & Graham, C. H.  
566 (2008). Predicting species distributions across the Amazonian and Andean regions using  
567 remote sensing data. *Journal of Biogeography*, **35**, 1160-1176.

568

569 Bwangoy, J. R. B., Hansen, M. C., Roy, D. P., De Grandi, G., & Justice, C. O. (2010). Wetland  
570 mapping in the Congo Basin using optical and radar remotely sensed data and derived  
571 topographical indices. *Remote Sensing of Environment*, **114**, 73-86.

572

573 Carreiras, J. M., Jones, J., Lucas, R. M., & Shimabukuro, Y. E. (2017), Mapping major land  
574 cover types and retrieving the age of secondary forests in the Brazilian Amazon by  
575 combining single-date optical and radar remote sensing data. *Remote Sensing of*  
576 *Environment*, **194**, 16-32.

577

578 Chen, C. M., Hepner, G. F., & Forster, R. R. (2003), Fusion of hyperspectral and radar data  
579 using the IHS transformation to enhance urban surface features. *ISPRS Journal of*  
580 *photogrammetry and Remote Sensing*, **58**, 19-30.

581

582 Cartus, O., Santoro, M., Schullius, C., & Li, Z. (2011). Large area forest stem volume  
583 mapping in the boreal zone using synergy of ERS-1/2 tandem coherence and MODIS  
584 vegetation continuous fields. *Remote Sensing of Environment*, **115**, 931-943.

585

586 Cracraft, J. (1987). Species concepts and the ontology of evolution. *Biology and philosophy*,  
587 **2**, 329-346.

588

589 Culbert, P. D., Radeloff, V. C., Flather, C. H., Kellndorfer, J. M., Rittenhouse, C. D., & Pidgeon, A.  
590 M. (2013). The influence of vertical and horizontal habitat structure on nationwide  
591 patterns of avian biodiversity. *The Auk*, **130**, 656-665.

592

593 Dong, J., Xiao, X., Chen, B., Torbick, N., Jin, C., Zhang, G., & Biradar, C. (2013). Mapping  
594 deciduous rubber plantations through integration of PALSAR and multi-temporal Landsat  
595 imagery. *Remote Sensing of Environment*, **134**, 392-402.

596 Enright, N. J., Fontaine, J. B., Bowman, D. M., Bradstock, R. A., & Williams, R. J. (2015).  
597 Interval squeeze: altered fire regimes and demographic responses interact to threaten  
598 woody species persistence as climate changes. *Frontiers in Ecology and the Environment*,  
599 **13**, 265-272.

600

601 Fitzpatrick, B. M., Ryan, M. E., Johnson, J. R., Corush, J., & Carter, E. T. (2015). Hybridization  
602 and the species problem in conservation. *Current Zoology*, **61**, 206-216.

603

604 Fu, B., Wang, Y., Campbell, A., Li, Y., Zhang, B., Yin, S., Xing, Z., & Jin, X. (2017), Comparison of  
605 object-based and pixel-based Random Forest algorithm for wetland vegetation mapping  
606 using high spatial resolution GF-1 and SAR data. *Ecological Indicators*, **73**, 105-117.

607

608 Gala, T. S., & Melesse, A. M. (2012). Monitoring prairie wet area with an integrated  
609 LANDSAT ETM+, RADARSAT-1 SAR and ancillary data from LIDAR. *Catena*, **95**, 12-23.

610

611 Gavier-Pizarro, G. I., Kuemmerle, T., Hoyos, L. E., Stewart, S. I., Huebner, C. D., Keuler, N. S., &  
612 Radeloff, V. C. (2012). Monitoring the invasion of an exotic tree (*Ligustrum lucidum*) from  
613 1983 to 2006 with Landsat TM/ETM+ satellite data and Support Vector Machines in  
614 Córdoba, Argentina. *Remote Sensing of Environment*, **122**, 134-145.

615 Geijzendorffer, I. R., Regan, E. C., Pereira, H. M., Brotons, L., Brummitt, N., Gavish, Y., ... &  
616 Schmeller, D. S. (2016). Bridging the gap between biodiversity data and policy reporting  
617 needs: An Essential Biodiversity Variables perspective. *Journal of Applied Ecology*, **53**,  
618 1341-1350.

619

620 Ghulam, A., Porton, I., & Freeman, K. (2014), Detecting subcanopy invasive plant species in  
621 tropical rainforest by integrating optical and microwave (InSAR/PolInSAR) remote sensing  
622 data, and a decision tree algorithm. *ISPRS Journal of Photogrammetry and Remote Sensing*,  
623 **88**, 174-192.

624

625 Goetz, A. F. H., Vane, G., Solomon, J., & Rock, B. (1985). Imaging spectrometry for earth  
626 remote sensing. *Science*, **228**, 1147-1152.

627

628 Haack, B. N., Solomon, E. K., Bechdol, M. A., & Herold, N. D. (2002), Radar and optical data  
629 comparison/integration for urban delineation: a case study. *Photogrammetric Engineering  
630 and Remote Sensing*, **68**, 1289-1296.

631

632 Hamdan, O., Hasmadi, I. M., & Aziz, H. K. (2014), Combination of SPOT-5 and ALOS PALSAR  
633 images in estimating aboveground biomass of lowland Dipterocarp forest. *IOP Conference  
634 Series: Earth and Environmental Science*, **18**, 012016.

635

636 Hamilton, S. K., Kellndorfer, J., Lehner, B., & Tobler, M. (2007). Remote sensing of floodplain  
637 geomorphology as a surrogate for biodiversity in a tropical river system (Madre de Dios,  
638 Peru). *Geomorphology*, **89**, 23-38.

639

640 He, K. S., Bradley, B. A., Cord, A. F., Rocchini, D., Tuanmu, M. N., Schmidtlein, S., Turner, W.,  
641 Wegmann, M. & Pettorelli, N. (2015), Will remote sensing shape the next generation of  
642 species distribution models? *Remote Sensing in Ecology and Conservation*, **1**, 4-18.

643

644 Hégarat-Masclé, S., Bloch, I., & Vidal-Madjar, D. (1998). Introduction of neighborhood  
645 information in evidence theory and application to data fusion of radar and optical images  
646 with partial cloud cover. *Pattern recognition*, **31**, 1811-1823.

647

648 Hergoualc'h, K., Gutiérrez-Vélez, V. H., Menton, M., & Verchot, L. V. (2017). Characterizing  
649 degradation of palm swamp peatlands from space and on the ground: An exploratory study  
650 in the Peruvian Amazon. *Forest Ecology and Management*, **393**, 63-73.

651

652 Hong, G., Zhang, Y., & Mercer, B. (2009), A wavelet and IHS integration method to fuse high  
653 resolution SAR with moderate resolution multispectral images. *Photogrammetric*  
654 *Engineering & Remote Sensing*, **75**, 1213-1223.

655

656 Hong, G., Zhang, A., Zhou, F., & Brisco, B. (2014), Integration of optical and synthetic  
657 aperture radar (SAR) images to differentiate grassland and alfalfa in Prairie area.  
658 *International Journal of Applied Earth observation and geoinformation*, **28**, 12-19.

659

660 Hu, X., Tao, C. V., & Hu, Y. (2004), Automatic road extraction from dense urban area by  
661 integrated processing of high resolution imagery and lidar data. *International Archives of*  
662 *Photogrammetry, Remote Sensing and Spatial Information Sciences*, **35**, B3.

663

664 Hyde, P., Dubayah, R., Walker, W., Blair, J. B., Hofton, M., & Hunsaker, C. (2006). Mapping  
665 forest structure for wildlife habitat analysis using multi-sensor (LiDAR, SAR/InSAR, ETM+,  
666 Quickbird) synergy. *Remote Sensing of Environment*, **102**, 63-73.

667

668 Ismail, R., Kassier, H., Chauke, M., Holecz, F., & Hattingh, N. (2015). Assessing the utility of  
669 ALOS PALSAR and SPOT 4 to predict timber volumes in even-aged Eucalyptus plantations  
670 located in Zululand, South Africa. *Southern Forests: a Journal of Forest Science*, **77**, 203-211.

671

672 Joppa, L. N., O'Connor, B., Visconti, P., Smith, C., Geldmann, J., Hoffmann, M., ... & Burgess, N.  
673 D. (2016), Filling in biodiversity threat gaps. *Science*, **352**, 416-418.

674

675 Joshi, N., Baumann, M., Ehammer, A., Fensholt, R., Grogan, K., Hostert, P., ... & Waske, B.  
676 (2016), A review of the application of optical and radar remote sensing data fusion to land  
677 use mapping and monitoring. *Remote Sensing*, **8**, 70.

678

679 Keith, S. A., Webb, T. J., Böhning-Gaese, K., Connolly, S. R., Dulvy, N. K., Eigenbrod, F., ... &  
680 Isaac, N. J. (2012) What is macroecology? *Biology Letters*, DOI:10.1098.

681



682 Keith, D. A., Rodríguez, J. P., Rodríguez-Clark, K. M., Nicholson, E., Aapala, K., Alonso, A., ... &  
683 Zambrano-Martínez, S. (2013), Scientific foundations for an IUCN Red List of Ecosystems.  
684 *PLOS one*, **8**, e62111.

685

686 Kelndorfer, J. M., Walker, W. S., LaPoint, E., Kirsch, K., Bishop, J., & Fiske, G. (2010),  
687 Statistical fusion of Lidar, InSAR, and optical remote sensing data for forest stand height  
688 characterization: A regional-scale method based on LVIS, SRTM, Landsat ETM+, and  
689 ancillary data sets. *Journal of Geophysical Research*, **115**, G00E08.

690

691 Kemp, W. M., Boynton, W. R., Adolf, J. E., Boesch, D. F., Boicourt, W. C., Brush, G., ... &  
692 Harding, L. W. (2005). Eutrophication of Chesapeake Bay: historical trends and ecological  
693 interactions. *Marine Ecology Progress Series*, **303**, 1-29.

694

695 Kuenzer, C., Ottinger, M., Wegmann, M., Guo, H., Wang, C., Zhang, J., Dech, S. & Wikelski, M.  
696 (2014), Earth observation satellite sensors for biodiversity monitoring: potentials and  
697 bottlenecks. *International Journal of Remote Sensing*, **35**, 6599-6647.

698

699 Lahat, D., Adali, T., & Jutten, C. (2015), Multimodal data fusion: an overview of methods,  
700 challenges, and prospects. *Proceedings of the IEEE*, **103**, 1449-1477.

701

702 Laurin, G. V., Liesenberg, V., Chen, Q., Guerriero, L., Del Frate, F., Bartolini, A., ... & Valentini,  
703 R. (2013). Optical and SAR sensor synergies for forest and land cover mapping in a tropical

704 site in West Africa. *International Journal of Applied Earth Observation and Geoinformation*,  
705 **21**, 7-16.

706

707 Lehmann, E. A., Caccetta, P. A., Zhou, Z. S., McNeill, S. J., Wu, X., & Mitchell, A. L. (2011), Joint  
708 processing of Landsat and ALOS-PALSAR data for forest mapping and monitoring. *IEEE*  
709 *Transactions on Geoscience and Remote Sensing*, **50**, 55-67.

710

711 Lehmann, E. A., Caccetta, P., Lowell, K., Mitchell, A., Zhou, Z. S., Held, A., Milne, T. & Tapley, I.  
712 (2015), SAR and optical remote sensing: Assessment of complementarity and  
713 interoperability in the context of a large-scale operational forest monitoring system.  
714 *Remote Sensing of Environment*, **156**, 335-348.

715

716 Leung, Y., Liu, J., & Zhang, J. (2014), An improved adaptive intensity-hue-saturation  
717 method for the fusion of remote sensing images. *IEEE Geoscience and Remote Sensing*  
718 *Letters*, **11**, 985-989.

719

720 Leutner, B. & Horning, N. (2016), RStoolbox: Tools for Remote Sensing Data Analysis. R  
721 package version 0.1.4. Available at: <https://CRAN.R-project.org/package=RStoolbox>,  
722 retrieved 10/04/2016.

723

724 Lisini, G., Gamba, P., Dell'Acqua, F., & Holecz, F. (2011), First results on road network  
725 extraction and fusion on optical and SAR images using a multi-scale adaptive approach.  
726 *International Journal of Image and Data Fusion*, **2**, 363-375.

727

728 Liu, M., Liu, X., Li, J., Ding, C., & Jiang, J. (2014). Evaluating total inorganic nitrogen in coastal  
729 waters through fusion of multi-temporal RADARSAT-2 and optical imagery using random  
730 forest algorithm. *International Journal of Applied Earth Observation and Geoinformation*, **33**,  
731 192-202.

732

733 Lu, D., Li, G., Moran, E., Dutra, L., & Batistella, M. (2011), A comparison of multisensor  
734 integration methods for land cover classification in the Brazilian Amazon. *GIScience &*  
735 *Remote Sensing*, **48**, 345-370.

736

737 Lu, D., Li, G., Moran, E., & Kuang, W. (2014), A comparative analysis of approaches for  
738 successional vegetation classification in the Brazilian Amazon. *GIScience & Remote Sensing*,  
739 **51**, 695-709.

740

741 Lucas, R. M., Clewley, D., Accad, A., Butler, D., Armston, J., Bowen, ... & Seabrook, L. (2014),  
742 Mapping forest growth and degradation stage in the Brigalow Belt Bioregion of Australia  
743 through integration of ALOS PALSAR and Landsat-derived foliage projective cover data.  
744 *Remote Sensing of Environment*, **155**, 42-57.

745

746 Ludäscher, B., Altintas, I., Bowers, S., Cummings, J., Critchlow, T., Deelman, E., ... & Klasky, S.  
747 (2009). Scientific process automation and workflow management. *Scientific Data*  
748 *Management: Challenges, Existing Technology, and Deployment, Computational Science*  
749 *Series*, **230**, 476-508.

750

751 Mace, G. M., Hails, R. S., Cryle, P., Harlow, J., & Clarke, S. J. (2015), Review: towards a risk  
752 register for natural capital. *Journal of Applied Ecology*, **52**, 641-653.

753

754 Maillard, P., Alencar-Silva, T., & Clausi, D. A. (2008). An evaluation of Radarsat-1 and ASTER  
755 data for mapping veredas (palm swamps). *Sensors*, **8**, 6055-6076.

756

757 Marvin, D. C., Koh, L. P., Lynam, A. J., Wich, S., Davies, A. B., Krishnamurthy, R., Stokes, E.,  
758 Starkey, R. & Asner, G. P. (2016), Integrating technologies for scalable ecology and  
759 conservation. *Global Ecology and Conservation*, **7**, 262-275.

760

761 McCauley, J. F., Schaber, G. G., Breed, C. S., Grolier, M. J., Haynes, C. V., Issawi, B., Elachi, C. &  
762 Blom, R. (1982), Subsurface valleys and geoarcheology of the eastern Sahara revealed by  
763 shuttle radar. *Science*, **218**, 1004-1020.

764

765 McGill, B. J., Enquist, B. J., Weiher, E., & Westoby, M. (2006). Rebuilding community ecology  
766 from functional traits. *Trends in ecology & evolution*, **21**, 178-185.

767

768 McDowall, R. M. (2004), What biogeography is: a place for process. *Journal of Biogeography*,  
769 **31**, 345-351.

770

771 Michener, W. K., & Jones, M. B. (2012), Ecoinformatics: supporting ecology as a data-  
772 intensive science. *Trends in ecology & evolution*, **27**, 85-93.

773

774 Morel, A. C., Fisher, J. B., & Malhi, Y. (2012). Evaluating the potential to monitor  
775 aboveground biomass in forest and oil palm in Sabah, Malaysia, for 2000–2008 with  
776 Landsat ETM+ and ALOS-PALSAR. *International Journal of Remote Sensing*, **33**, 3614-3639.

777

778 Myneni, R. B., Ramakrishna, R., Nemani, R., & Running, S. W. (1997). Estimation of global  
779 leaf area index and absorbed PAR using radiative transfer models. *IEEE Transactions on*  
780 *Geoscience and remote sensing*, **35**, 1380-1393.

781

782 Myers, N., Mittermeier, R. A., Mittermeier, C. G., Da Fonseca, G. A., & Kent, J. (2000).  
783 Biodiversity hotspots for conservation priorities. *Nature*, **403**, 853.

784

785 Naidoo, L., Mathieu, R., Main, R., Wessels, K., & Asner, G. P. (2016), L-band Synthetic  
786 Aperture Radar imagery performs better than optical datasets at retrieving woody  
787 fractional cover in deciduous, dry savannahs. *International Journal of Applied Earth*  
788 *Observation and Geoinformation*, **52**, 54-64.

789

790 Nicholson, E., Keith, D. A., & Wilcove, D. S. (2009), Assessing the threat status of ecological  
791 communities. *Conservation Biology*, **23**, 259-274.

792

793 Noss, R. F. (1990). Indicators for monitoring biodiversity: a hierarchical approach.  
794 *Conservation biology*, **4**, 355-364.

795

796 Pajares, G., & De La Cruz, J. M. (2004), A wavelet-based image fusion tutorial. *Pattern*  
797 *recognition*, **37**, 1855-1872.

798

799 Palumbo, I., Rose, R. A., Headley, R. M., Nackoney, J., Vodacek, A., & Wegmann, M. (2017),  
800 Building capacity in remote sensing for conservation: present and future challenges.  
801 *Remote Sensing in Ecology and Conservation*, **3**, 21-29.

802

803 Pasher, J., Smith, P. A., Forbes, M. R., & Duffe, J. (2013). Terrestrial ecosystem monitoring in  
804 Canada and the greater role for integrated earth observation. *Environmental Reviews*, **22**,  
805 179-187.

806

807 Pereira, H. M., Ferrier, S., Walters, M., Geller, G. N., Jongman, R. H. G., Scholes, R. J., ... &  
808 Coops, N. C. (2013). Essential biodiversity variables. *Science*, **339**, 277-278.

809

810 Pettorelli, N., Vik, J. O., Mysterud, A., Gaillard, J. M., Tucker, C. J., & Stenseth, N. C. (2005).  
811 Using the satellite-derived NDVI to assess ecological responses to environmental change.  
812 *Trends in ecology & evolution*, **20**, 503-510.

813

814 Pettorelli, N., Laurance, W. F., O'Brien, T. G., Wegmann, M., Nagendra, H., & Turner, W.  
815 (2014a), Satellite remote sensing for applied ecologists: opportunities and challenges.  
816 *Journal of Applied Ecology*, **51**, 839-848.

817

818 Pettorelli, N., Safi, K., & Turner, W. (2014b). Satellite remote sensing, biodiversity research  
819 and conservation of the future. *Phil Trans Royal Soc B*, 369: 20130190.

820

821 Pettorelli, N., Wegmann, M., Skidmore, A., Múcher, S., Dawson, T. P., Fernandez, M., ... &  
822 Jongman, R. H. (2016). Framing the concept of satellite remote sensing essential  
823 biodiversity variables: challenges and future directions. *Remote Sensing in Ecology and*  
824 *Conservation*, 2, 122-131.

825

826 Pettorelli, N., Schulte to Bühne, H., Tulloch, A., Dubois, G., Macinnis-Ng, C., Queirós, A. M., ... &  
827 Sonnenschein, R. (2017). Satellite remote sensing of ecosystem functions: opportunities,  
828 challenges and way forward. *Remote Sensing in Ecology and Conservation*. In press.

829

830 Pickett, S. T., & Cadenasso, M. L. (2002). The ecosystem as a multidimensional concept:  
831 meaning, model, and metaphor. *Ecosystems*, 5, 1-10.

832

833 Poggio, L., & Gimona, A. (2017), Assimilation of optical and radar remote sensing data in 3D  
834 mapping of soil properties over large areas. *Science of The Total Environment*, 579, 1094-  
835 1110.

836

837 Pohl, C. (1999), Tools and methods for fusion of images of different spatial resolution.  
838 *International Archives of Photogrammetry and Remote Sensing*, 32, part 7-4-3 W6.

839

840 Pohl, C., & Van Genderen, J. L. (1998), Review article multisensor image fusion in remote  
841 sensing: concepts, methods and applications. *International journal of remote sensing*, **19**,  
842 823-854.

843

844 Pohl, C., & Yen, T. L. (2014) Compilation of a remote sensing image fusion atlas. *35th Asian*  
845 *Conference of Remote Sensing (ACRS)*, 1-6.

846

847 Polychronaki, A., Gitas, I. Z., & Minchella, A. (2014), Monitoring post-fire vegetation  
848 recovery in the Mediterranean using SPOT and ERS imagery. *International Journal of*  
849 *Wildland Fire*, **23**, 631-642.

850

851 Prates-Clark, C. D. C., Saatchi, S. S., & Agosti, D. (2008). Predicting geographical distribution  
852 models of high-value timber trees in the Amazon Basin using remotely sensed data.  
853 *Ecological Modelling*, **211**, 309-323.

854

855 Pressey, R. L., & Bottrill, M. C. (2008), Opportunism, threats, and the evolution of systematic  
856 conservation planning. *Conservation Biology*, **22**, 1340-1345.

857

858 Reiche, J., Souza, C. M., Hoekman, D. H., Verbesselt, J., Persaud, H., & Herold, M. (2013).  
859 Feature level fusion of multi-temporal ALOS PALSAR and Landsat data for mapping and  
860 monitoring of tropical deforestation and forest degradation. *IEEE Journal of Selected Topics*  
861 *in Applied Earth Observations and Remote Sensing*, **6**, 2159-2173.

862



863 Reiche, J., Verbesselt, J., Hoekman, D., & Herold, M. (2015a), Fusing Landsat and SAR time  
864 series to detect deforestation in the tropics. *Remote Sensing of Environment*, **156**, 276-293.  
865

866 Reiche, J., de Bruin, S., Hoekman, D., Verbesselt, J., & Herold, M. (2015b), A Bayesian  
867 approach to combine Landsat and ALOS PALSAR time series for near real-time  
868 deforestation detection. *Remote Sensing*, **7**, 4973-4996.  
869

870 Rignot, E., Salas, W. A., & Skole, D. L. (1997). Mapping deforestation and secondary growth  
871 in Rondônia, Brazil, using imaging radar and Thematic Mapper data. *Remote Sensing of*  
872 *Environment*, **59**, 167-179.  
873

874 Robertson, B. P., Gardner, J. P., & Savage, C. (2015), Macrobenthic–mud relations strengthen  
875 the foundation for benthic index development: a case study from shallow, temperate New  
876 Zealand estuaries. *Ecological Indicators*, **58**, 161-174.  
877

878 Sangster, G. (2014). The application of species criteria in avian taxonomy and its  
879 implications for the debate over species concepts. *Biological Reviews*, *89*(1), 199-214.  
880

881 Santoro, M., Shvidenko, A., McCallum, I., Askne, J., & Schmullius, C. (2007), Properties of  
882 ERS-1/2 coherence in the Siberian boreal forest and implications for stem volume retrieval.  
883 *Remote sensing of environment*, **106**, 154-172.  
884

885 Shea, K., Roxburgh, S. H., & Rauschert, E. S. (2004), Moving from pattern to process:  
886 coexistence mechanisms under intermediate disturbance regimes. *Ecology letters*, **7**, 491-  
887 508.

888

889 Souza-Filho, P. W. M., Goncalves, F. D., Rodrigues, S. W. P., Costa, F. R., & Miranda, F. P.  
890 (2009), Multi-sensor data fusion for geomorphological and environmental sensitivity index  
891 mapping in the Amazonian mangrove coast, Brazil. *Journal of Coastal Research*, **56**, 1592-  
892 1596.

893

894 Stroppiana, D., Azar, R., Calò, F., Pepe, A., Imperatore, P., Boschetti, M., ... & Lanari, R. (2015).  
895 Integration of optical and SAR data for burned area mapping in Mediterranean Regions.  
896 *Remote Sensing*, **7**, 1320-1345.

897

898 Tansley, A. G. (1935). The use and abuse of vegetational concepts and terms. *Ecology*, **16**,  
899 284-307.

900

901 Tempfli, K., Kerle, N., Huurneman, G. C., & Janssen, L. L. (2009), Principles of remote  
902 sensing. *The International Institute for Geo-Information Science and Earth Observation (ITC)*.  
903 *Enschede, Netherlands*.

904

905 Treuhaft, R. N., Law, B. E., & Asner, G. P. (2004), Forest attributes from radar  
906 interferometric structure and its fusion with optical remote sensing. *BioScience*, **54**, 561-  
907 571.

908

909 Tulloch, V. J., Tulloch, A. I., Visconti, P., Halpern, B. S., Watson, J. E., Evans, M. C., ... &  
910 Possingham, H.P. (2015), Why do we map threats? Linking threat mapping with actions to  
911 make better conservation decisions. *Frontiers in Ecology and the Environment*, **13**, 91-99.

912

913 Turner, W., Rondinini, C., Pettorelli, N., Mora, B., Leidner, A. K., Szantoi, Z., ...& Woodcock, C.  
914 (2015), Free and open-access satellite data are key to biodiversity conservation. *Biological*  
915 *Conservation*, **182**, 173-176.

916

917 UNSD SEEA-EEA (2013), System of Environmental-Economic Accounting 2012:  
918 Experimental Ecosystem Accounting. Accessible at  
919 [http://unstats.un.org/unsd/envaccounting/eea\\_white\\_cover.pdf](http://unstats.un.org/unsd/envaccounting/eea_white_cover.pdf), retrieved on  
920 10/04/2017.

921

922 van der Wal, D., & Herman, P. M. (2007), Regression-based synergy of optical, shortwave  
923 infrared and microwave remote sensing for monitoring the grain-size of intertidal  
924 sediments. *Remote Sensing of Environment*, **111**, 89-106.

925

926 Vihervaara, P., Auvinen, A. P., Mononen, L., Törmä, M., Ahlroth, P., Anttila, S., ... &  
927 Koskelainen, M. (2017). How Essential Biodiversity Variables and remote sensing can help  
928 national biodiversity monitoring. *Global Ecology and Conservation*, **10**, 43-59.

929

930 Vivone, G., Alparone, L., Chanussot, J., Dalla Mura, M., Garzelli, A., Licciardi, G. A., ... & Wald,  
931 L. (2015). A critical comparison among pansharpening algorithms. *IEEE Transactions on*  
932 *Geoscience and Remote Sensing*, **53**, 2565-2586.

933

934 Wald, L. (1999), Some terms of reference in data fusion. *IEEE Transactions on geoscience*  
935 *and remote sensing*, **37**, 1190-1193.

936

937 Walker, W. S., Kelndorfer, J. M., LaPoint, E., Hoppus, M., & Westfall, J. (2007), An empirical  
938 InSAR-optical fusion approach to mapping vegetation canopy height. *Remote Sensing of*  
939 *Environment*, **109**, 482-499.

940

941 Wang, C., Qi, J., Moran, S., & Marsett, R. (2004). Soil moisture estimation in a semiarid  
942 rangeland using ERS-2 and TM imagery. *Remote Sensing of Environment*, **90**, 178-189.

943

944 Wang, C., & Qi, J. (2008). Biophysical estimation in tropical forests using JERS-1 SAR and  
945 VNIR imagery. II. Aboveground woody biomass. *International Journal of Remote Sensing*,  
946 **29**, 6827-6849.

947

948 Wang, X. Y., Guo, Y. G., He, J., & Du, L. T. (2016), Fusion of HJ1B and ALOS PALSAR data for  
949 land cover classification using machine learning methods. *International Journal of Applied*  
950 *Earth Observation and Geoinformation*, **52**, 192-203.

951

952 Ward, D. P., Petty, A., Setterfield, S. A., Douglas, M. M., Ferdinands, K., Hamilton, S. K., &  
953 Phinn, S. (2014). Floodplain inundation and vegetation dynamics in the Alligator Rivers  
954 region (Kakadu) of northern Australia assessed using optical and radar remote sensing.  
955 *Remote Sensing of Environment*, **147**, 43-55.

956

957 Waske, B., & Benediktsson, J. A. (2007), Fusion of support vector machines for classification  
958 of multisensor data. *IEEE Transactions on Geoscience and Remote Sensing*, **45**, 3858-3866.

959

960 Wegmann, M. & Leutner, B. (2016) Introduction to Remote Sensing and GIS. In: M.  
961 Wegmann, B. Leutner, S. Dech (eds) *Remote Sensing and GIS for Ecologists*. Pelagic  
962 Publishing, Exeter, UK.

963

964 Wolter, P. T., & Townsend, P. A. (2011), Multi-sensor data fusion for estimating forest  
965 species composition and abundance in northern Minnesota. *Remote Sensing of*  
966 *Environment*, **115**, 671-691.

967

968 Wulder, M. A., Masek, J. G., Cohen, W. B., Loveland, T. R., & Woodcock, C. E. (2012), Opening  
969 the archive: How free data has enabled the science and monitoring promise of Landsat.  
970 *Remote Sensing of Environment*, **122**, 2-10.

971

972 Yonghong, J. (1998), Fusion of Landsat TM and SAR image based on principal component  
973 analysis. *Remote Sensing Technology and Application*, **13**, 46-49.

974

975 Zhang, Y., Pulliainen, J., Koponen, S., & Hallikainen, M. (2002). Application of an empirical  
976 neural network to surface water quality estimation in the Gulf of Finland using combined  
977 optical data and microwave data. *Remote sensing of environment*, **81**, 327-336.

978

979 Zhang, J. (2010), Multi-source remote sensing data fusion: status and trends. *International*  
980 *Journal of Image and Data Fusion*, **1**, 5-24.

981

982

983 **Figures and Tables**

984 **Box 1:** Definitions of key terms relating to remote sensing and data fusion.

985 **Table 1** Overview of current applications of multispectral-radar SRS data fusion for species  
986 and ecosystem monitoring , as well as biodiversity threat detection via (A) image fusion  
987 (P= pixel-based fusion; O=object-based fusion) or (B) decision-level data fusion  
988 (integration). (\*) identifies studies that explicitly compare multispectral-radar image  
989 fusion/data integration to approaches which use either data alone.

990 **Figure 1:** Schematic overview of multispectral-radar SRS data fusion techniques. The  
991 parameter of interest can be a categorical variable, like land cover, or a continuous  
992 variable, like species richness. In pixel-level fusion, the original pixel values of radar and  
993 multispectral imagery are combined to yield new, derived pixel values. Object-based fusion  
994 refers to 1) using radar and multispectral imagery is input into an object-based image  
995 segmentation algorithm, or 2) segmenting each type of imagery separately before  
996 combining them. Finally, decision-level fusion corresponds to the process of quantitatively  
997 combining multispectral and radar imagery to derive the parameter of interest (by e.g.  
998 combining them in a regression model, or classification algorithm).

999 **Figure 2:** Overview of the advantages and drawbacks of the most common multispectral-  
1000 radar SRS image fusion techniques, as well as examples for open-source software to  
1001 implement them.

1002 **Figure 3:** Spatial resolution and launch date of freely available SRS data with global  
1003 coverage from active, long-term missions. Included are only missions which are currently

1004 active. The relative lack of radar missions is due to the fact that most missions with open-  
1005 access data policies are not active (e.g. JERS-1, ALOS PALSAR, ERS-1/2) whilst imagery  
1006 from active radar missions is often behind a paywall (ALOS-2, RADARSAT-1/2, TerraSAR-  
1007 X).

1008 **Figure 4:** Roadmap for identifying and generating Essential Biodiversity Variables based  
1009 on SRS (SRS-EBVs) supported by data fusion. The ecology/conservation science community  
1010 and the remote sensing community each contribute their intradisciplinary expertise to a  
1011 collaborative, interdisciplinary process in which biodiversity monitoring requirements are  
1012 matched with appropriate SRS data and analysis techniques. The outcome of this process is  
1013 a consensus about which SRS-EBVs will benefit from data fusion approaches, as well as the  
1014 SRS data required and recommendations for data fusion techniques. This then feeds into  
1015 the operationalisation stage, which involves the two science communities as well as policy-  
1016 makers, to enable the production and use of SRS-EBVs, and which includes validation,  
1017 endorsement, repeated generation, storage, dissemination of SR\_EBVs.

1018 .



### **Box 1: Definitions of key terms relating to satellite remote sensing and data fusion**

**Band:** Defined section in the visible and near-infrared part of the electromagnetic spectrum (Wegmann & Leutner 2016).

**Data fusion:** A formal framework in which data from different sources (and hence, sensors) is combined (“alliance des données”) to obtain information of greater quality (Wald 1999).

**Hyperspectral remote sensing:** Type of remote sensing which records radiance in a high number of sections of the electromagnetic spectrum (typically 100s of bands), allowing the reconstruction of a contiguous reflectance profile (Goetz et al. 1985).

**Image fusion:** A type of data fusion, in which images from different sources are combined into a new image. The aim is to create an image that retains salient information whilst minimizing artefacts or distortion.

**Integration:** We use “integration” to refer to decision-level data fusion, emphasising that whilst no new imagery is produced, the SRS data is systematically combined in a quantitative framework.

**Leaf Area Index (LAI):** One-sided green leaf area per unit ground area (Myneni et al. 1997).

**Light Detection and Ranging (LiDAR):** A type of active remote sensor which emits pulses of light and measures the proportion of the signal which is reflected; based on this

information, the three-dimensional location of the object that reflected the light can be reconstructed.

**Multispectral remote sensing:** Measuring the amount of electromagnetic radiation in a limited number of bands (typically less than 10) in the visible and infrared part of the spectrum. Widely used spaceborne multispectral sensors include the Landsat and MODIS missions. Different from hyperspectral remote sensing (see above).

**Normalised Difference Vegetation index (NDVI):** A common vegetation index based on reflectance in the red and the near-infrared part of the spectrum, sensitive to the amount of photosynthetically active vegetation in a given area (Pettorelli et al. 2005).

**Pan-sharpening:** Fusing multispectral imagery with a panchromatic image of higher spatial resolution to increase the spatial resolution of the former whilst preserving its spectral information (“colour”) (Vivone et al. 2015).

**Radar remote sensing:** Emitting a signal of electromagnetic radiation with a defined wavelength in the microwave spectrum and measuring the intensity and wavephase of the returning signal. Widely used spaceborne radar sensors include ALOS PALSAR and RADARSAT-2.

**Table 1**

**(A)**

	<b>Variable</b>	<b>Proxy</b>	<b>Multispectral sensor (spatial resolution)</b>	<b>Radar sensor (wavelength; spatial resolution)</b>	<b>Spatial scale</b>	<b>Reference</b>	<b>Type of data fusion</b>
<b>Species-level biodiversity</b>	Species distribution	Distribution of alfalfa stands ( <i>Medicago salvatica</i> )	MODIS (250m)	RADARSAT-2 (C-band; 50m)	50,000 km <sup>2</sup>	Hong et al. 2014*	P
	Community composition	Relative basal area of 10 tree species and 2 tree genera	Landsat 5 TM (30m), SPOT 5 (10m)	Radarsat-1 (C-band, ca. 27m), ALOS PALSAR (L-band, ca. 12.5m)	360 km <sup>2</sup>	Wolter & Townsend 2011*	P
<b>Ecosystem-level biodiversity</b>	Ecosystem distribution	Distribution of different forest types, including different successional stages	Landsat 5 TM (30m)	RADARSAT-2 (C-band, 8m), ALOS PALSAR (L-band, 12.5m)	3,100 km <sup>2</sup>	Lu et al. 2011*	P
			Landsat 5 TM (30m)	ALOS PALSAR (L-band, 12.5m)	3,000 km <sup>2</sup>	Lu et al. 2014*	P
			Landsat 5 TM and Landsat 7 ETM+ (30m)	ALOS PALSAR (25m)	ca. 370,000 km <sup>2</sup>	Lucas et al. 2014	O
	Distribution of vegetation and/or geomorphology types in a wetland ecosystem		Landsat 7 ETM+(15m and 30m)	JERS-1 (L-band, 100m), SRTM (C-band, ca. 90m)	31,000 km <sup>2</sup>	Hamilton et al. 2007	O
			Landsat 5 TM (30m)	RADARSAT-1 (C-band, 33x27 m)	1,600 km <sup>2</sup>	Souza-Filho et al. 2009	P
			Landsat 5 TM (30m)	ALOS PALSAR (L-band, 20m), ERS-1/2 (C-band, 30m)	250 km <sup>2</sup> /34,000 km <sup>2</sup> respectively	Bourgeau-Chavez et al. 2009, 2016	O
			GF-1 (2m and 8m)	ALOS PALSAR (L-band, 14m)	250 km <sup>2</sup>	Fu et al. 2017*	P/O

				RADARSAT-2 (C-band, 6.3m x 5.2m)			
	Vertical ecosystem structure	Canopy height	Landsat 5 TM and Landsat 7 ETM+ (30m)	SRTM (C-band, ca. 30m)	62,000 km <sup>2</sup>	Walker et al. 2007*	O
			Landsat 7 ETM+ (30m)	SRTM (C-band, ca. 30m)	110,000 km <sup>2</sup>	Kellndorfer et al. 2010	O
		Aboveground biomass	Landsat 7 ETM+ (30m)	ALOS PALSAR (L-band, 16m resampled)	31,000 km <sup>2</sup>	Basuki et al. 2013	P
<b>Threats to biodiversity</b>	Deforestation	Historic deforestation events	Landsat 7 ETM+ (30m)	ALOS PALSAR (L-band, 25m)	30 km <sup>2</sup>	Reiche et al. 2015a*	P

**(B)**

	Variable	Proxy	Multispectral sensor (spatial resolution)	Radar sensor (wavelength; spatial resolution)	Spatial scale	Reference	Type of data fusion
<b>Species-level biodiversity</b>	Species distribution	Bird species	NLCD (from Landsat TM; 30m)	SIR-C (both L and C band, 25m)	ca. 1,200 km <sup>2</sup>	Bergen et al. 2007*	Genetic Algorithm For Rule Set Production
			MODIS-derived LAI and Vegetation Continuous Fields (500m)	QuickScat (X-band, 1km)	17.8 million km <sup>2</sup>	Buermann et al. 2008	Species Distribution Model
	Subcanopy plant species	Landsat 5 TM and 7 ETM+ (30m), GeoEye-1 (1.64m), IKONOS (4m)	RADARSAT-2 (L-band, 8m), ALOS PALSAR (L-band, 12.5m)	22.3 km <sup>2</sup>	Ghulam et al. 2014	Decision tree algorithm	
	Tropical tree species		MODIS-derived NDVI, LAI, Vegetation continuous fields (500m)	QuickScat (X-band, 1km)	ca. 7.5 million km <sup>2</sup>	Prates-Clark et al. 2008	Species Distribution Model
			MODIS-derived LAI and Vegetation Continuous Fields	QuickScat (X-band, 2.25km), SRTM (C-band, ca. 30m)	17.8 million km <sup>2</sup>	Buermann et al. 2008	Species Distribution Model

			(500m)				
<b>Ecosystem-level biodiversity</b>	Ecosystem distribution	Wetland vegetation types	Landsat TM and ETM+ (57m)	JERS-1 (L-band, 100m), SRTM (C-band, 30m)	1.2 million km <sup>2</sup>	Bwangoy et al. 2010	Classification trees
			GF-1 (2m and 8m)	ALOS PALSAR (L-band, 14m) RADARSAT-2 (C-band, 6.3m x 5.2m)	250 km <sup>2</sup>	Fu et al. 2017*	Random forest
		Forest types	Landsat TM (30m), AVNIR-2 (10m)	ALOS PALSAR (L-band, 15m)	7,750 km <sup>2</sup>	Laurin et al. 2013	Maximum Likelihood & Neural Networks Classifiers
			SPOT 1 or 2 (20m)	ERS (C-band, 12.6m)	Not reported	Hégart-Masclé et al. 1998	Dempster-Shafner fusion
			Landsat TM (30m)	SIR-C (C and L-band, 12.5m)	ca. 520 km <sup>2</sup>	Rignot et al. 1997*	Rule-based classification
	Horizontal ecosystem structure	Forest stem density	MODIS vegetation continuous field product (500m)	ERS1-2 (C-band, 25 m or 50m depending on location)	1.5 million km <sup>2</sup>	Cartus et al. 2011	Exponential SIBERIA model, semi-empirical Interferometric Water Cloud Model
		Woody canopy cover	Landsat TM (30m)	ALOS PALSAR (L-band, 12.5m)	ca. 31,000 km <sup>2</sup>	Naidoo et al. 2016*	Random Forest
		Sediment grain size	Landsat TM (30m)	ERS-1 and 2 (C-band, 12.5m)	ca. 100 km <sup>2</sup>	van der Wal & Herman 2007*	Multiple least-squares regression
		Soil density, composition	Sentinel-2, Landsat, MODIS (rescaled to 100m)	Sentinel-1 (C-band, rescaled to 100m)	ca. 78,000 km <sup>2</sup>	Poggio & Gimona 2017*	Generalised additive model
		Soil moisture	Landsat 5 TM (30m)	ERS-2 (C-band, not reported)	400 km <sup>2</sup>	Wang et al. 2004	Quantitative modelling
	Vertical ecosystem structure	Biomass	JERS VNIR (18m)	JERS-1 SAR (L-band, 60m)	6700 km <sup>2</sup>	Wang & Qi 2008	Quantitative modelling
			Landsat 7 ETM+ (30m)	ALOS PALSAR (L-band, resampled to 30m)	107 km <sup>2</sup>	Attarchi & Gloaguen 2014*	Linear regression
			SPOT-5 (5m)	ALOS PALSAR (L-band, 25m)	1,090 km <sup>2</sup>	Hamdan et al. 2014*	Linear regression
Timber volume		SPOT-4 (resampled to 100m)	ALOS PALSAR (L-band, resampled to 100m)	ca. 360 km <sup>2</sup>	Ismail et al. 2015	Linear regression	

	Ecosystem function	Fire dynamics extent of burned areas	Landsat 5 TM (30m)	Envisat ASAR (C-band, 60m x 80m)	ca. 90,000 km <sup>2</sup>	Stroppiana et al. 2015*	Fuzzy decision algorithm
		Wetland inundation dynamics	Landsat 5TM (30m)	ALOS PALSAR (L-band, 100m)	ca. 3,400 km <sup>2</sup>	Ward et al. 2014*	Classification tree modelling
	Landsat 7 ETM+ (30m)		RADARSAT-1 (C-band, 12.5m)	ca. 15 km <sup>2</sup>	Gala & Melesse 2012	Post-classification combination	
<b>Threats to biodiversity</b>	Eutrophication	Chlorophyll- $\alpha$ , Secchi disk depth, suspended sediment concentration, turbidity	Landsat 5 TM (30m)	ERS-2 (C-band, 12.5m)	ca. 29,600 km <sup>2</sup>	Zhang et al. 2002*	Artificial neural networks
		Inorganic nitrogen concentration	HJ-1 (30m)	RADARSAT-2 (C-band, 12 x 8m)	ca. 2,500 km <sup>2</sup>	Liu et al. 2014*	Random Forest
	Forest degradation	Degradation of palm swamp	Landsat 5 TM (30m)	ALOS PALSAR (L-band, 12.5m)	3,500 km <sup>2</sup>	Hergoualc'h et al. 2017	Random Forest
	Deforestation	Plantation expansion	Landsat TM and ETM+ (30m)	ALOS PALSAR (L-band, 50m)	3,400 km <sup>2</sup>	Dong et al. 2013	Post-classification combination
		Deforestation events	Landsat TM (30m)	SIR-C (L and C-band, 12.5m), JERS-1 (L-band, 12.5 m)	ca. 520 km <sup>2</sup>	Rignot et al. 1997*	Rule-based classification
			Landsat 5 and 7 (30m)	ALOS PALSAR (L-band, 25m)	ca. 7,800 km <sup>2</sup>	Reiche et al. 2013*	Rule-based classification
			Landsat 7 ETM+ (30m)	ALOS PALSAR (L-band, 25m)	ca. 96 km <sup>2</sup>	Reiche et al. 2015b*	Bayesian time series modeling
			Landsat MSS/TM/ETM+ (30m)	ALOS PALSAR (L-band; 25m)	3,300 km <sup>2</sup>	Lehmann et al. 2011*	Bayesian time series modeling

**Figure 1**

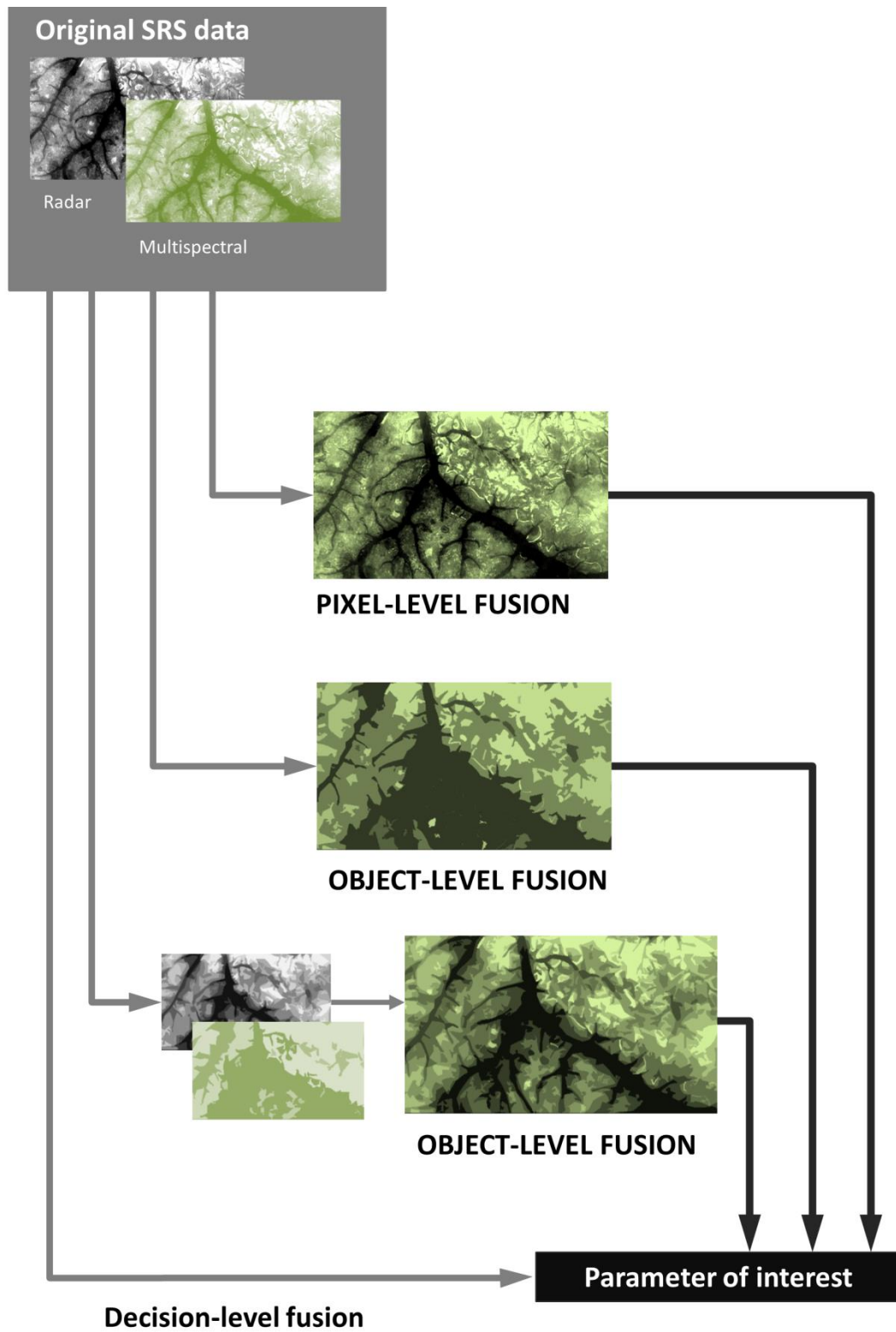


Figure 2

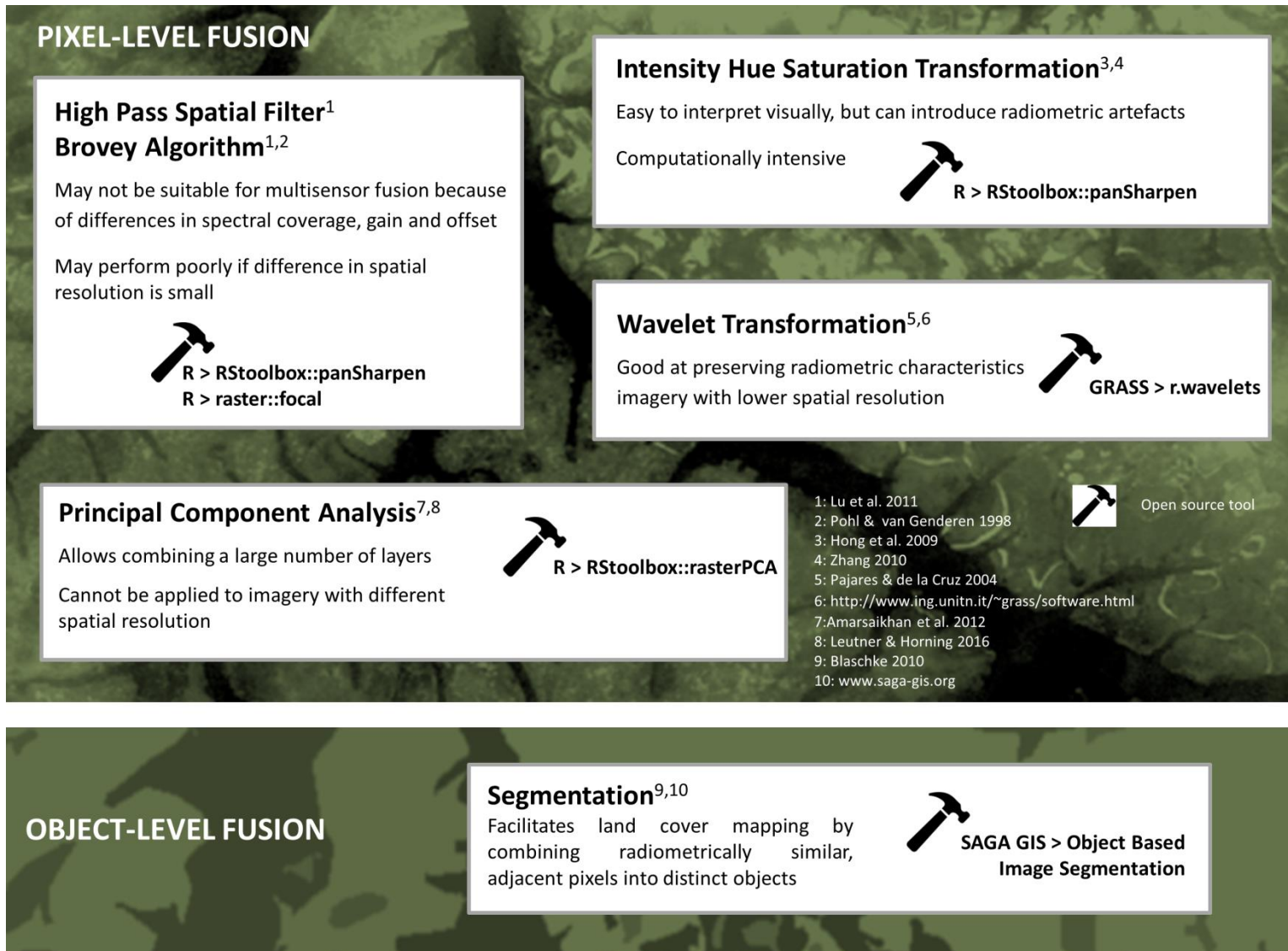
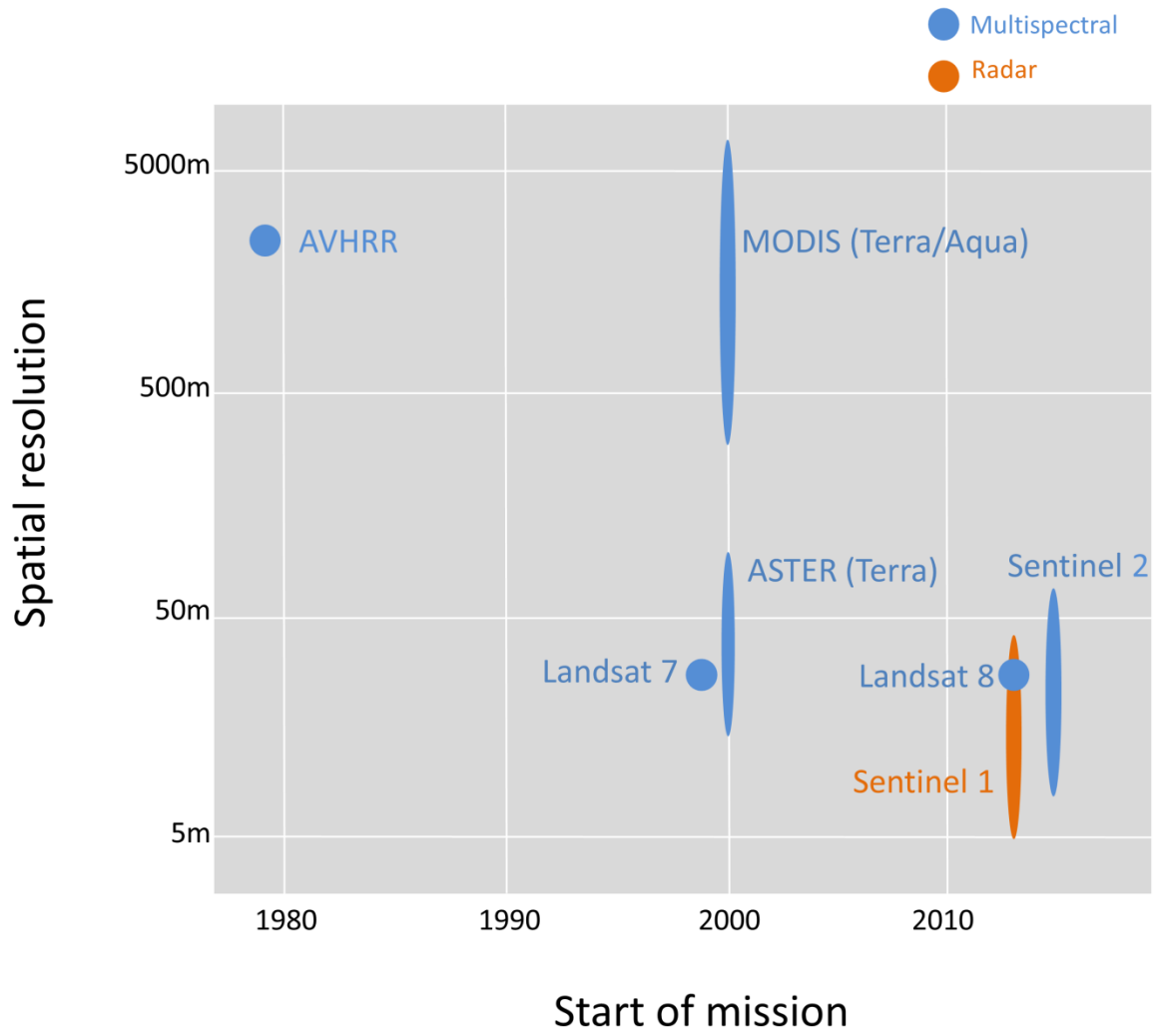




Figure 3



**Figure 4**

